Clinical Case Collection

11 cases where where dynamic imaging with Dual Source CT is making a difference

siemens-healthineers.com/dual-source-ct

SIEMENS Healthineers

Only this page contains new content, all the cases are reuses.

Introduction

2–3% is the annual increase of hepatocellular carcinoma (HCC) death rate.[1] HCC is frequently diagnosed late and lacks curative therapy for advanced stages.

At the same time, identification and treatment of vascular malformations is a challenging endeavor for physicians, especially given the great concern and anxiety created for patients and their families. For those challenges, morphologic imaging alone may not be sufficient.

Thanks to unrivaled power and precision, dynamic imaging with Dual Source CT enables our customers to obtain high-quality results in every situation easily and conveniently. Our revolutionary technology is the right match for even the most challenging and advanced imaging applications.

Explore how users around the world have employed the large coverage of Dual Source CT to advance the possibilities of dynamic imaging.

Explore the untapped potential of dynamic imaging with Dual Source CT.

[1] *Weiyi W, et al. (2020): Advances in the early diagnosis of hepatocellular carcinoma.*

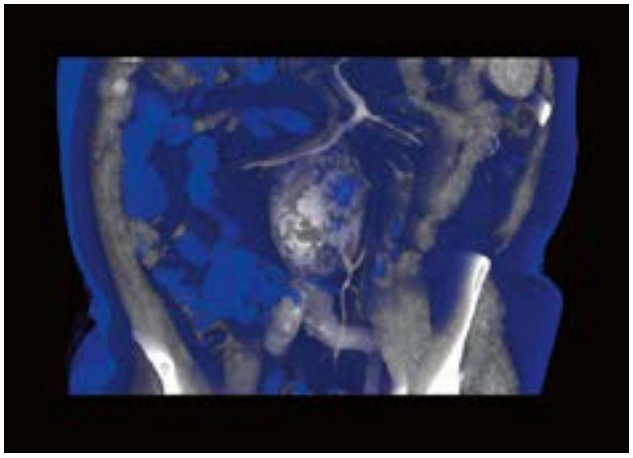

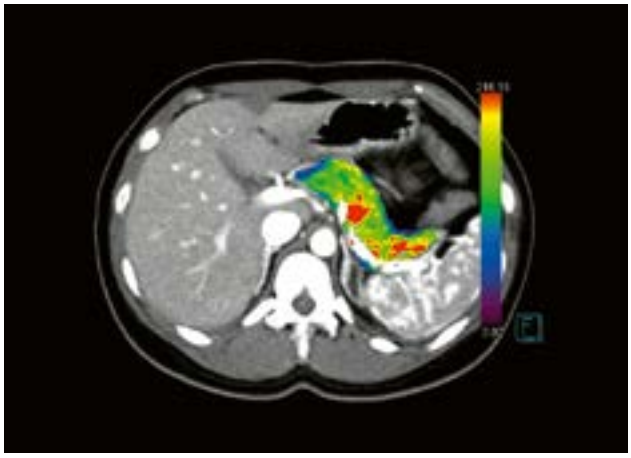

Dynamic CT Angiography

04 Discovery of a type II endoleak after EVAR in a patient with renal insufficiency using dynamic 4D CT angiography

06 Adaptive 4D Spiral CT angiography for the diagnosis of a capillary hemangioma

08 Follow-up on post-bronchial artery embolization

12 Multiple, enlarged and tortuous pulmonary vessels – a straightforward diagnosis?

14 Time resolved CT angiography in patients after EVAR

16 Isolated common iliac artery aneurysm – complicated by peripheral artery insufficiency in the lower limb?

Body Perfusion

18 CT Volume Perfusion imaging in a case of suspected pancreatic cancer

20 CT imaging of insulinomas – biphasic or dynamic?

22 Pre-operative detection of an isoattenuating pancreatic insulinoma in Volume Perfusion CT

24 Volumetric Perfusion CT for early assessment of response to anti-angiogenic therapy in metastatic renal cell carcinoma

26 Volume Perfusion CT during hepatic arteriography of hepatocellular carcinoma

Discovery of a type II endoleak after EVAR in a patient with renal insufficiency using dynamic 4D CT angiography

Holger Haubenreisser, MD
Institute of Clinical Radiology and Nuclear Medicine, University Medical Centre Mannheim, Medical Faculty Mannheim, Heidelberg University, Germany

History

A 72-year-old male patient with poor kidney function (GFR 40 mL/min) was admitted to the hospital with a suspected endoleak after an endovascular aneurysm repair (EVAR) of the abdominal aorta. A dynamic 4D CT angiography (CTA) was requested to confirm the endoleak and to specify its type.

Diagnosis

CT images showed an abdominal aortic aneurysm (AAA) and a stent within it, placed during EVAR. Proof of an endoleak (Figs. 1 and 2) was seen in the delayed phase, as was the aneurysmal feeder artery (Fig. 3). A type II endoleak was confirmed.

Comments

Due to the patient's poor kidney function, the examination was completed with only 12 cc of contrast, at a 60% dilution (total injected volume 20 cc), followed by a 30 cc saline chaser, both with a 5 cc/s injection rate. This was achieved by conducting the scan at 70 kV, to close the gap to the k-edge and enhance the contrast, as well as by using a dynamic 4D scan protocol for a shorter scan range than a standard abdominal CTA. The multiple acquisition time points of the dynamic scan make overtaking or missing the bolus highly unlikely. The images were viewed on a 4D viewer. It was seen clearly that the contrast flow into the aneurysm (the endoleak) was delayed in comparison with that into the aorta. This is an indirect sign of a type II rather than a type I endoleak. Further evaluation of the same dataset revealed a small feeder artery, thus confirming the diagnosis. ●

Examination Protocol

Scanner	**SOMATOM Force**		
Scan area	Abdomen	Rotation time	0.25 s
Scan length	222 mm	Slice collimation	48 × 1.2 mm
Scan mode	Adaptive 4D Spiral	Slice width	1.5 mm
Scan direction	Shuttle	Reconstruction increment	1.0 mm
Scan time	36 s	Reconstruction kernel	Bv36
Tube voltage	70 kV		
Effective mAs	200 mAs	**Contrast**	400 mg/mL
Effective dose	13.6 mSv	Volume	12 mL (20 mL diluted to 60%) + 30 mL saline
$CTDI_{vol}$	43.46 mGy	Flow rate	5 mL/s
DLP	905 mGy*cm	Start delay	8 s

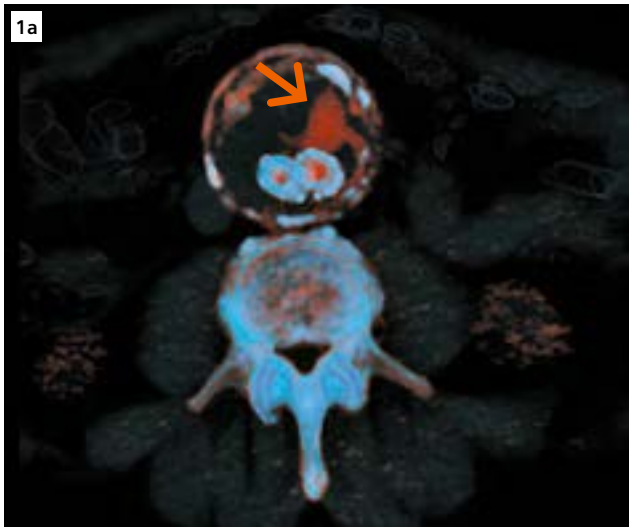

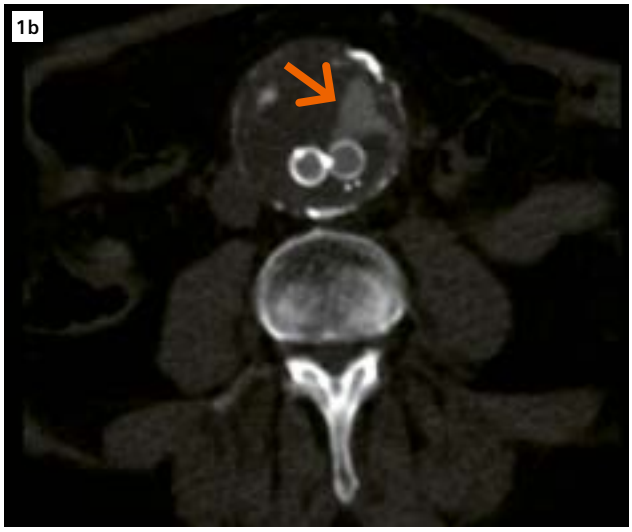

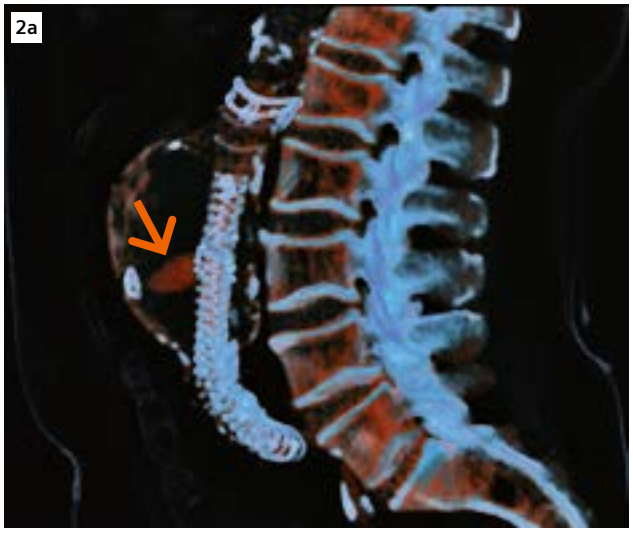

1-2 **Axial (Fig. 1) and sagittal (Fig. 2) views of VRT (a) and MPR (b) images show the endoleak (arrows).**

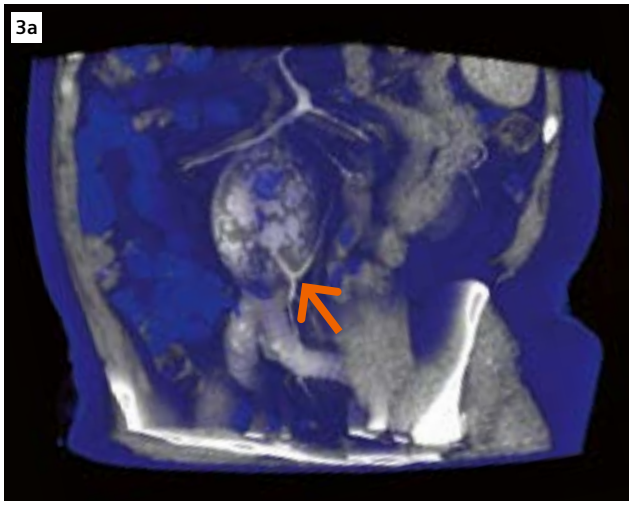

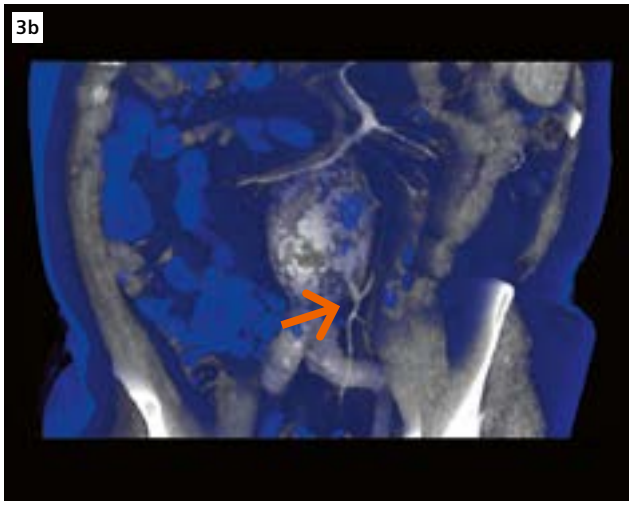

3 **VRT image demonstrates the feeder artery (arrows) to the aneurysm and thus confirms a type II endoleak.**

Adaptive 4D Spiral CT angiography for the diagnosis of a capillary hemangioma

Xiaoping-ming Fang, MD; Xiao-yun Hu, MD; Hong-wei Chen, MD; Ping-yan Qian, MD; Gang-feng Hu, MD; Hui-jun Lu, MD; Chenwei Li, MD[1]
Department of Radiology, Wuxi People's Hospital Affiliated to Nanjing Medical University, Wuxi, P. R. China
[1]Siemens Healthineers, China

History

A 29-year-old female patient presented herself to the hospital with a tumor on the ulnar side of her left ring finger. The tumor had appeared a month earlier, small and asymptomatic. It however progressed in size and caused discomfort and occasional bleeding. Physical examination revealed a firm, non-pulsatile subcutaneous tumor near the distal interphalangeal joint. The capillary return and the movement of the finger were normal. The skin covering the tumor appeared normal and there was no sensory loss.

Diagnosis

Non-contrast CT images showed a soft tissue tumor, measuring 1.8 cm × 1.7 cm, on the ulnar side of the distal left ring finger. The tumor was well defined and clearly separated from the phalanx (Fig. 1). CT Angiography (CTA) images acquired with the Adaptive 4D Spiral demonstrated significant and homogeneous enhancement of the tumor with its feeding artery, along with two draining veins (Fig. 2–3). These results suggested a vascular tumor or a vessel-originated tumor. The patient underwent surgery and the pathology report confirmed a capillary hemangioma.

Comments

Vascular abnormalities of the hand are infrequent and capillary hemangiomas of digital arteries are particularly rare. It is difficult to differentiate a hemangioma from a soft tissue lesion, such as an abscess, cyst, or neuroma, when the tumor is non-pulsatile, and the typical symptoms of arterial insufficiency (pain, pallor, no pulse, and paresthesia) are not present. Normal radiographs are usually not helpful unless erosive bone changes are suspected. Although angiography and nuclear scanning have proved to be helpful, they are considered invasive with possible complications. Contrarily, a CTA examination is noninvasive and easily available. In this case, the advanced 4D Spiral CTA with dynamic scanning technique was used to demonstrate the feeding artery and draining veins, thus providing valuable information not only for the diagnosis but also for surgery. ●

Examination Protocol

Scanner	SOMATOM Definition Flash
Scan area	Hand
Scan mode	Adaptive 4D Spiral
Scan length	150 mm
Scan direction	Shuttle
Scan time	24 s
Tube voltage	100 kV
Effective mAs	120 mAs
$CTDI_{vol}$	100 mGy
DLP	1520 mGy*cm
Effective dose	1.2 mSv
Rotation time	0.285 s
Slice collimation	32 × 1.2 mm
Slice width	1.5 mm
Reconstruction increment	1.0 mm
Reconstruction kernel	B20f

Contrast	
Volume	50 mL
Flow rate	3.5 mL/s
Start delay	Bolus tracking

1 The VRT image shows that the tumor (arrow) is well defined and clearly separated from the phalanx.

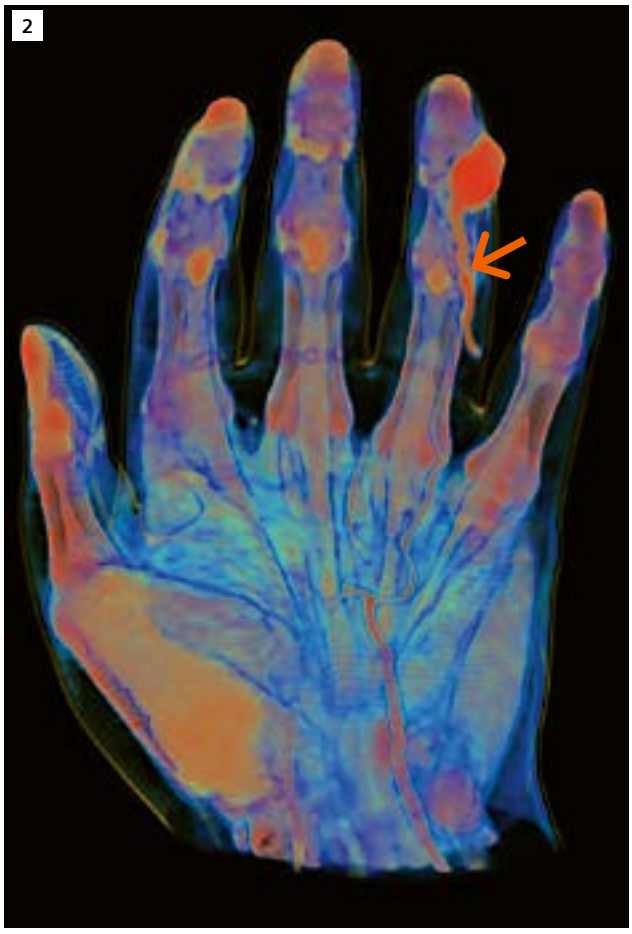

2 The VRT image shows one of two draining veins (arrow).

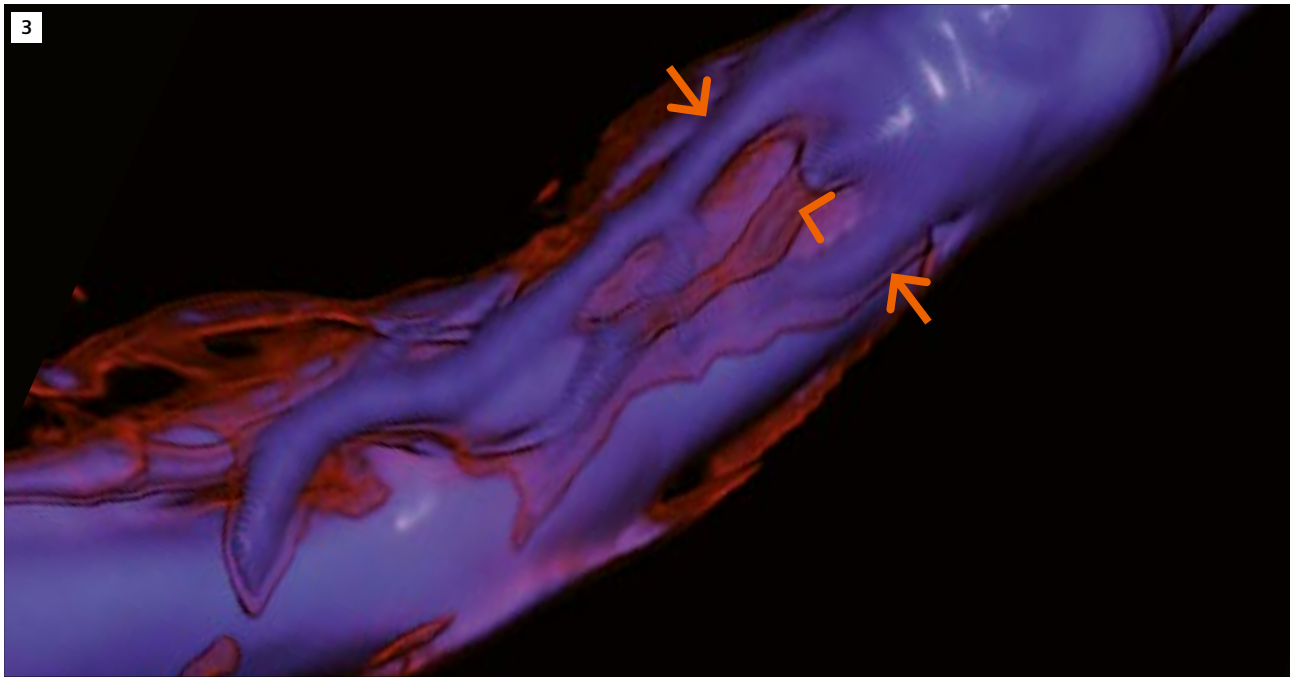

3 The VRT image demonstrates the feeding artery (arrowhead) and two draining veins (arrows).

Follow-up on post-bronchial artery embolization

Gang Wang, MD; Wei Song, MD; Xi Zhao, MD[1]
Department of Radiology, First People's Hospital of Yunnan Province, Kunming, P. R. China
[1]Siemens Healthineers, China

History

A 33-year-old male patient came to the hospital complaining of severe coughing with bloodstained sputum. He has been suffering from bronchiectasis and had undergone bronchial artery embolization (BAE) due to an acute hemoptysis three years ago. A 4D CT angiography (CTA) examination was requested for evaluation.

Diagnosis

CT images revealed typical imaging characteristics of bronchial dilation in both lungs associated with bronchiectasis (Fig. 1). Four bronchial arteries (BA) were identified – all issued from the aorta, with two on each side (Fig. 2). Three coils from the previous embolization were seen – two proximally in the recanalized upper right BA and another at the lesser curve of the aortic arch with no signs of BA recanalization. The lower right BA came anteriorly off the descending aorta at the level of T7, and appeared abnormally engorged and tortuous. The upper left BA came off the lesser curve of the aortic arch and divided into two branches – one with normal caliber going around the upper left pulmonary artery and another hypertrophied going tortuously along the lower left pulmonary artery. The lower left BA came anteriorly off the descending aorta at the level of T6 with a normal caliber. Bronchopulmonary shunting was suspected, could however be ruled out by inspecting time-resolved images (Fig. 3). No parenchymal hypervascularity or extravasation of the contrast agent was seen. The patient underwent pharmacotherapy and recovered uneventfully.

Comments

BAE for control of hemoptysis was first described in detail by Remy et al. in 1974.[1] It has become a mainstay in the treatment of hemoptysis. The common offenders can be BA, which vary considerably in their site of origin and subsequent

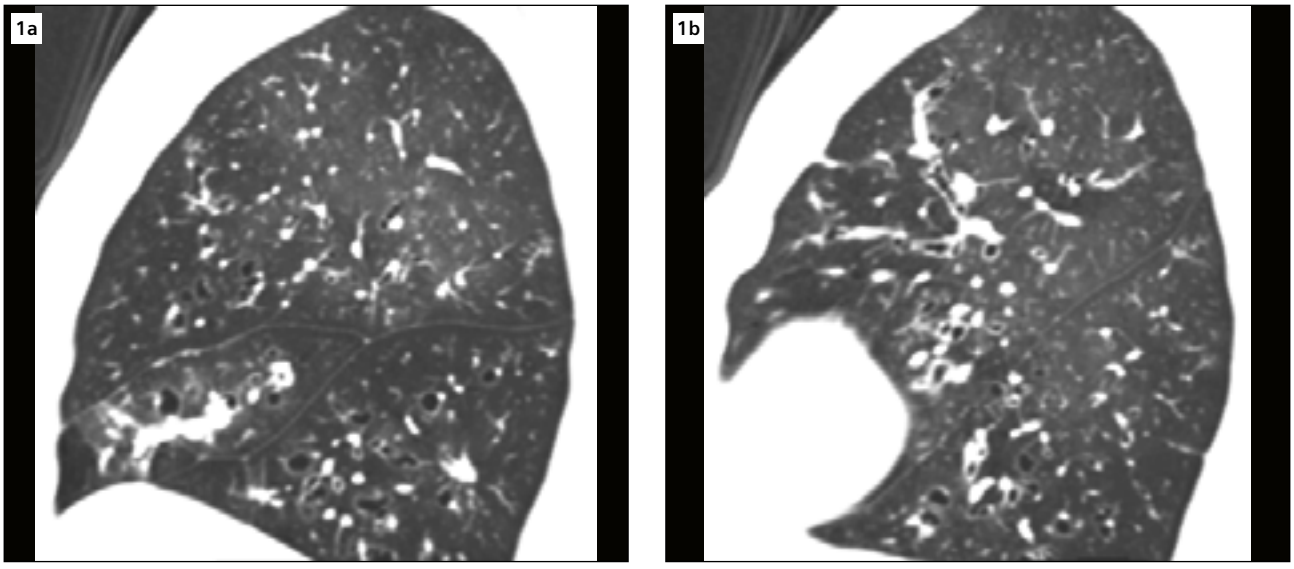

1 **Sagittal multiplanar reformations (1 mm) using phase volume acquired by Adaptive 4D Spiral show an increased bronchoarterial ratio, manifested by the signet ring sign, characterizing bronchial dilation associated with bronchiectasis in both lungs (Fig. 1a, right; and 1b, left).**

branching pattern, as well as the nonbronchial systemic arteries, which associate significantly with a higher rate of technical failure and unsuccessful embolization.[2] Aside from the typical complications associated with angiography, adverse events most frequently arise from unintentional, nontarget embolization, such as the most feared transverse myelitis due to nontarget embolization of the anterior spinal artery arising from the bronchial or intercostobronchial artery. Hemoptysis may recur due to recanalization of previously embolized vessels, missed culprit vessels, or recruitment of new collateral circulation.[3] Digital subtraction angiography (DSA) is primarily applied for BAE, whereas CT is performed to identify the underlying cause and extent of pulmonary diseases, to localize possible bleeding foci, to predict culprit vessels, to lay down the vascular roadmap prior to BAE, and to follow up. There are studies suggesting that multidetector CT may be more accurate than arteriography at delineating the origin and course of both the bronchial and nonbronchial systemic arteries, especially when combined with 3D reconstructions.[4,5] In this case, 80 kV was applied, which contributes not only to radiation dose reduction but also to contrast enhancement even though only 30 mL of contrast agent were used. The isotropic resolution provided by the Dual Source CT scanner helps achieve excellent image quality in visualizing detailed anatomical structures such as the bronchial arteries. Most importantly, the image series acquired by the Adaptive 4D Spiral scan facilitates a time-resolved inspection of the thoracic vascular system, which assists in ruling out a suspicious bronchopulmonary shunting. This is of great importance for interventionists, since an unintentional embolization of the occipital cortex could occur if such a shunt would exist. ●

Examination Protocol

Scanner	**SOMATOM Force**
Scan area	Thorax
Scan length	222.6 mm
Scan mode	Adaptive 4D Spiral
Scan direction	Shuttle
Scan time	28.5 s
Tube voltage	80 kV
Effective mAs	60 mAs
$CTDI_{vol}$	26.96 mGy
DLP	554.7 mGy*cm
Rotation time	0.25 s

Slice collimation	192 × 0.6 mm
Slice width	1.0 mm
Reconstruction increment	0.7 mm
Reconstruction kernel	Br36
Contrast	320 mg/mL
Volume	30 mL + 30 mL saline
Flow rate	5 mL/s
Start delay	12 s

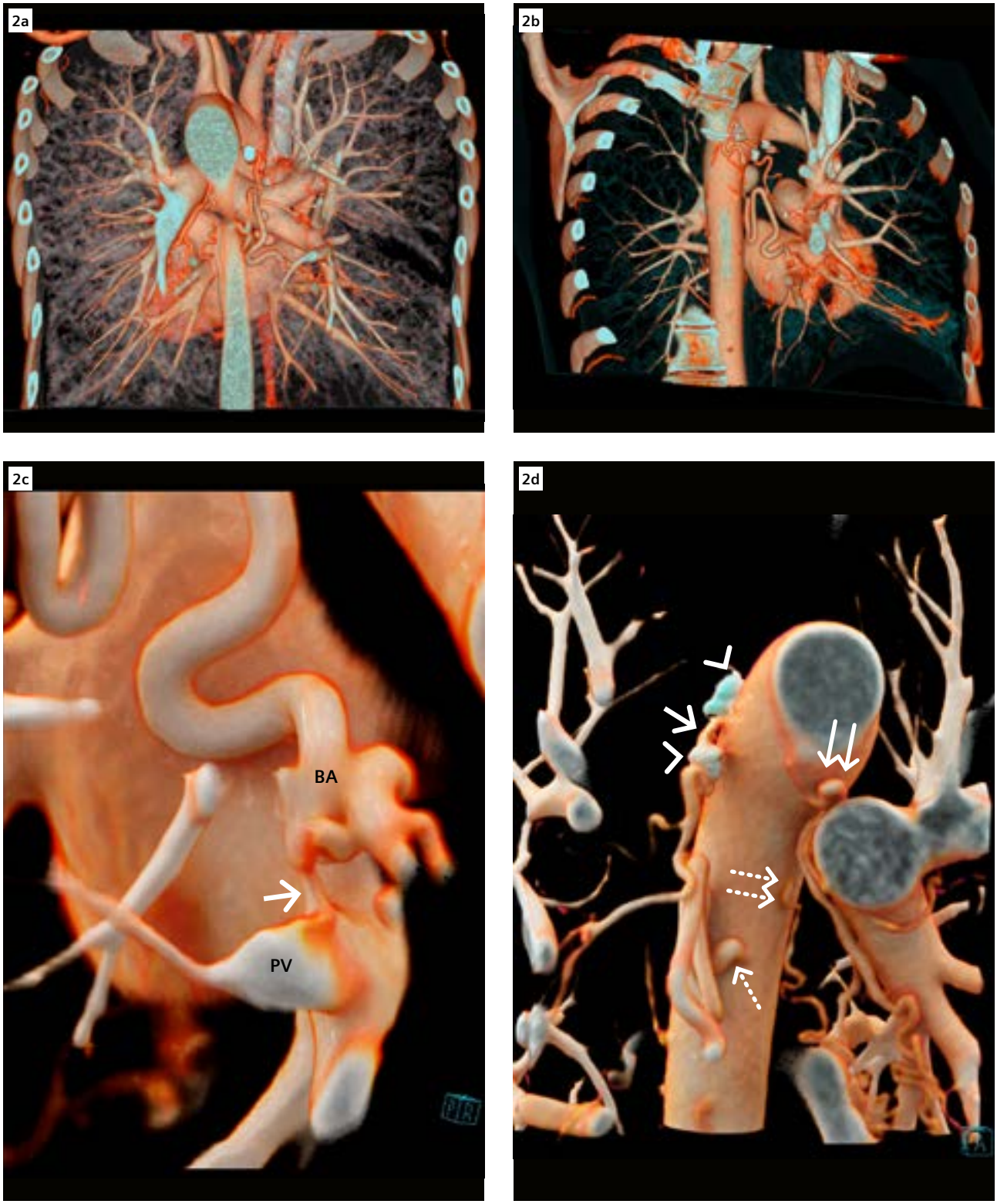

2 **Cinematic VRT images (Fig. 2a, posterior view; Fig. 2b and Fig. 2c, oblique views; Fig. 2d, anterior view) show the origins and the courses of the four identified BAs. Two coils (Fig. 2d, arrowheads) are seen in the recanalized upper right BA (Fig. 2d, arrow). The lower right BA is seen as abnormally engorged and tortuous (Fig. 2d, dotted arrow). The upper left BA (Fig. 2d, double arrows) branches into one with normal caliber and another hypertrophied. The lower left BA (Fig. 2d, double dotted arrows) shows a normal caliber. A suspicious bronchopulmonary shunting (Fig. 2c, arrow) is seen.**

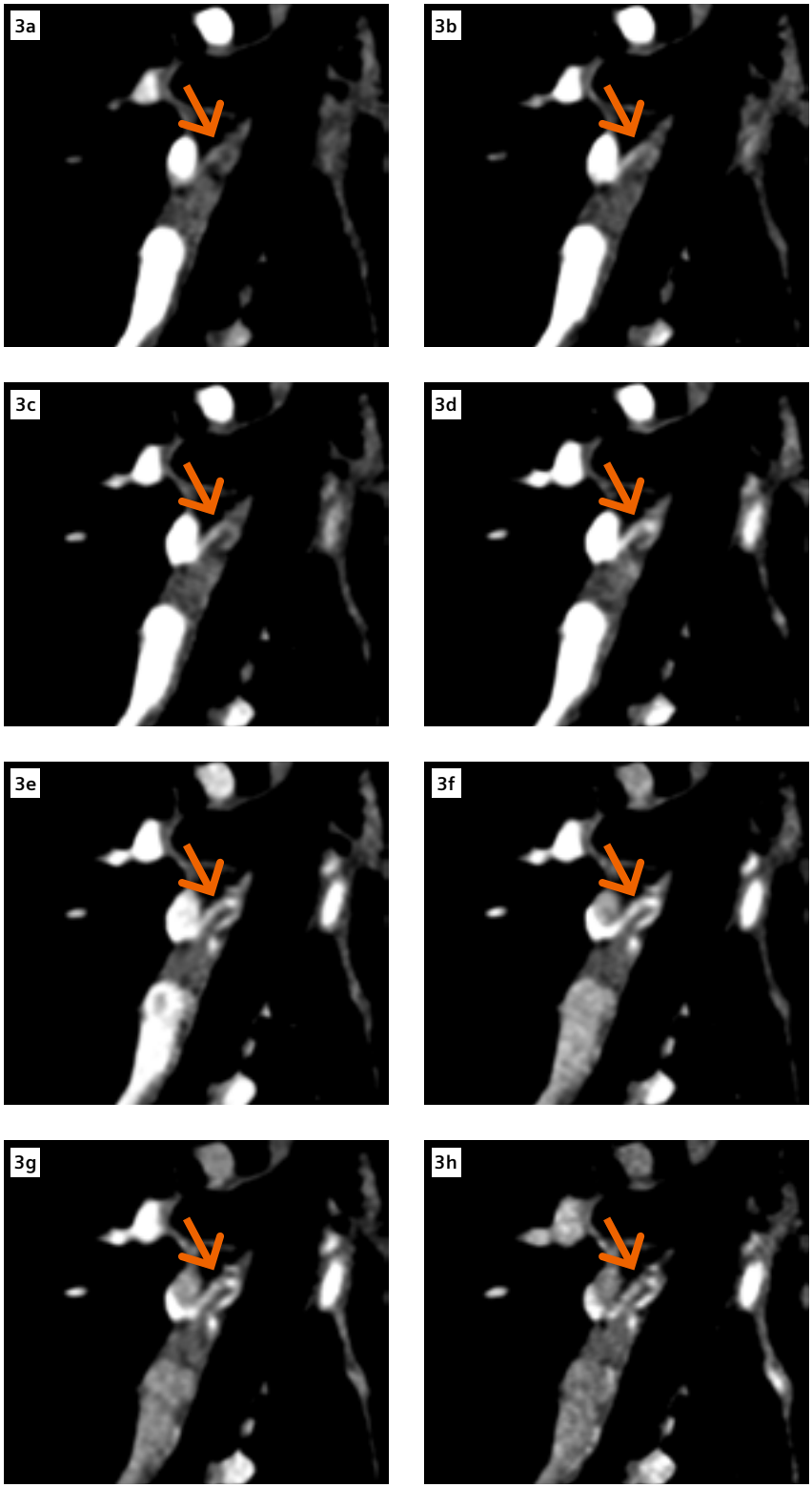

3 **Oblique MPR images show a dynamic view of a suspicious bronchopulmonary shunting (arrows). Image series are acquired with an interval of 1.5 seconds. Shunting is ruled out since there are no signs of refilling from the BA to the pulmonary vein.**

References

[1] Remy J, Voisin C, Dupuis C. Traitement des hémoptysies par embolization de la circulation systemique. Ann Radiol. 1974; 17:5–16.

[2] Chan VL, So LK, Lam JY, et al. Major haemoptysis in Hong Kong: aetiologies, angiographic findings and outcomes of bronchial artery embolisation. Int J Tuberc Lung Dis. 2009. Sep;13(9): 1167–1173.

[3] Razavi MK, Murphy K. Embolization of bronchial arteries with N-butyl cyanoacrylate for management of massive hemoptysis: a technical review. Tech Vasc Interv Radiol. 2007. Dec;10(4):276–282.

[4] Hartmann IJ, Remy-Jardin M, Menchini L, Teisseire A, Khalil C, Remy J. Ectopic origin of bronchial arteries: assessment with multidetector helical CT angiography. Eur Radiol. 2007. Aug;17(8):1943–1953.

[5] Remy-Jardin M, Bouaziz N, Dumont P, Brillet PY, Bruzzi J, Remy J. Bronchial and nonbronchial systemic arteries at multidetector row CT angiography: comparison with conventional angiography. Radiology 2004. Dec;233(3):741–749.

Multiple, enlarged and tortuous pulmonary vessels – a straightforward diagnosis?

Professor Helmut Ringl, MD; Paul Apfaltrer, MD, Division of General and Pediatric Radiology; Maria Schoder, MD, Division of Cardiovascular and Interventional Radiology; Department of Biomedical Imaging and Image guided Therapy, General Hospital of Vienna (AKH), Medical University of Vienna, Vienna, Austria

History

A 31-year-old female patient with a history of Crohn's disease presented herself with an abnormal finding on a plain film due to a recent pneumonia. CT of the chest was required for further evaluation.

Diagnosis

Adaptive 4D Spiral CTA images revealed atresia of several segmental pulmonary veins in both lower lobes with consecutive pulmonary varices, i.e. large venous collaterals that allowed venous drainage through adjacent segmental pulmonary veins.

The primary exam, a standard computed tomography pulmonary angiography (CTPA) showed multiple, tortuous and enlarged vessels in the periphery of both lower lobes. Even though the segmental atresia of several veins was recognized, the suspicion of coincidental pulmonary arteriovenous malformations (PAVMs) was raised due to similar contrasting of both arteries and veins. In addition, several small segmental arteries were shown in close vicinity of the enlarged tortuous vessels.

Comments

High-quality imaging is critical for a successful assessment and potential treatment of vascular malformations. Dependent upon their size, PAVMs are treated with embolotherapy to avoid complications, such as paradox embolism, whereas pulmonary varices usually require no treatment. Several imaging methods such as 4D-CTA, MRA and conventional angiography are used to assess the hemodynamic features of vascular lesions. In order to accurately identify the potential feeding arteries and draining veins of the suspected vascular malformation, an Adaptive 4D Spiral CTA mode was performed to generate detailed multiplanar images of the pulmonary vessels, as well as to allow accurate separation of the arterial and venous enhancement.

The scan range was planned to include both hilar and lower lobes. A test bolus was applied to acquire the time-to-density curve, which helped to determine the number of necessary scans. Informed consent was obtained from the patient prior to the Adaptive 4D Spiral CTA examination. Eight dynamic phases were acquired using 35 mL of contrast agent (Iomeron 400 mg) followed by saline chaser.

CTA images provided sufficient spatial and temporal resolution to completely separate pulmonary arterial and venous enhancement. The resulting images offered two arterial phases, three mixed phases and three venous phases. PAVMs were confidently ruled out since no venous enhancement was seen in the two arterial phases. Homogenous slow diffuse venous contrast filling was visible in the later phases.
The high spatial resolution of the SOMATOM Drive allowed easy depiction of the segmental venous atresia and the pathway of venous varices without segmentation. The Adaptive 4D Spiral CTA images contributed to a final distinct diagnosis for the patient at the dose of a standard CTPA of earlier days. ●

Examination Protocol

Scanner	SOMATOM Drive
Scan area	Thorax, lower lobes
Scan mode	Adaptive 4D Spiral
Scan length	147 mm
Scan direction	Shuttle
Scan time	10.3 s
Tube voltage	80 kV
Effective mAs	110 mAs
$CTDI_{vol}$	22.37 mGy
DLP	346 mGy*cm
Effective dose	4.8 mSv
Rotation time	0.28 s
Slice collimation	128 × 0.6 mm
Slice width	1.5 mm
Reconstruction increment	1.5 mm
Reconstruction kernel	B20f
Contrast	400 mg / mL
Volume	35 mL
Flow rate	4 mL / s
Start delay	7 s

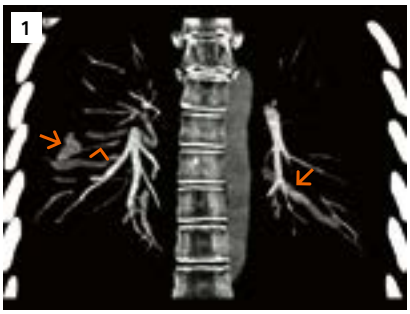

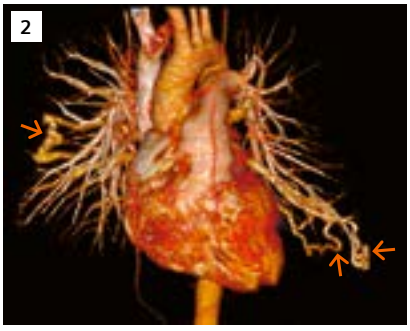

1 Coronal thin MIP of a standard CTA of the pulmonary arteries: It shows several large tortuous vessels in the periphery of both lower lobes (arrows) and suspected arterial feeder vessels (arrowhead).

2 Coronal VRT of a standard CTA of the pulmonary arteries: Several tortuous large vessels in the periphery of both lower lobes are depicted (arrows).

3a Thin MIP image from the first phase of the 8 phases performed with Adaptive 4D CTA mode shows contrast only in the pulmonary arteries of the right lower lobe.

3b Thin MIP image from the second phase shows high contrast in the pulmonary arteries only and a hint of diffuse enhancement in the pulmonary veins (arrow).

3c Thick MIP image from phase 7 shows high contrast in the pulmonary veins only, providing a clear image of the origin (arrowhead) and the extent (arrow) of the enlarged vessels. No segmentation was performed. Visualization is solely based on thin MIPs and a narrow contrast window.

4 Thin MIP of a late venous phase with high contrast in the pulmonary veins of the left lower lobe only, provides a view on the segmental vein atresia (arrowheads) and the varices (arrows) of the left lower lobe. Note that the pulmonary arteries are not visible on this image due to the high temporal resolution of the scan, the saline chaser and the use of a narrow contrast window.

References

[1] Anomalous unilateral single pulmonary vein: two cases mimicking arteriovenous malformations and a review of the literature. Hanson JM, Wood AM, Seymour R, Petheram IS. Australas Radiol. 2005 Jun;49(3):246-51. Review.

[2] Pulmonary vein varix: diagnosis with multi-slice helical CT. Vanherreweghe E, Rigauts H, Bogaerts Y, Meeus L. Eur Radiol. 2000;10(8):1315-7.

[3] Learning from the pulmonary veins. Porres DV, Morenza OP, Pallisa E, Roque A, Andreu J, Martínez M. Radiographics. 2013 Jul-Aug;33(4):999-1022. doi: 10.1148/rg.334125043. Review.

Time resolved CT angiography in patients after EVAR

Claudia Andres, MD; Borek Foldyna, MD; Christian Lücke, MD; Matthias Gutberlet, MD; Lukas Lehmkuhl, MD
Department of Diagnostic and Interventional Radiology, University of Leipzig, Heart Center, Leipzig, Germany

History

The patient presented himself for a follow-up examination after an endovascular implantation of an aorto-biiliacal Y-stentgraft due to an extant infrarenal aortic aneurysm in June 2004. The previous examination showed an increase in the size of the aneurysm sac (to max. 57 mm) and an endoleak type 1B. The endoleak was then shut out with an atrium stentgraft of the left common iliac artery. In the current contrast media duplex ultrasound, there was no hint of an endoleak or a perforation. For further assessment, a dynamic CT Angiography of the abdominal aorta was performed.

Diagnosis

The dynamic CT Angiography of the abdominal aorta demonstrated an unobtrusive stent prosthesis. Compared to the examination before stent implantation, the aneurysm sac showed a constant width with its maximal diameter being 57 mm. In the ventral part of the aneurysm sac, a type IIA endoleak was clearly defined, fed from the inferior mesenteric artery.

Comments

Contrary to the contrast media ultrasound examination, the dynamic CT Angiography helped determine the existence of an endoleak and delivered an explanation for the missing reduction in size of the aneurysm sac. Dynamic CTA may aid the physician in detecting the flow patterns of the different endoleaks by using multiple acquisitions at different time points and thereby increases both the sensitivity and the specificity for the detection of endoleaks. The gathered information concerning the dynamic of endoleaks considerably eases classification.[1] ●

References

[1] Lehmkuhl et al., Dynamic computed tomography angiography (dCTA) after abdominal aortic endovascular aneurysm repair (EVAR): Differences in contrast agent dynamics in the aorta and endoleaks – Preliminary results J Vase Interv Radial. 2012 Apr 9. [Epub ahead of print]

Examination Protocol

Scanner	SOMATOM Definition Flash
Scan area	Abdomen
Scan length	283 mm
Scan mode	Adaptive 4D Spiral
Scan direction	Shuttle
Scan time	54 s
Total scan phase	10
Tube voltage	80 kV
Effective mAs	120 mAs
$CTDI_{vol}$	28.47 mGy
DLP	629 mGy*cm
Effective dose	9.4 mSv
Rotation time	0.285 s
Slice collimation	128 × 0.6 mm
Slice width	1.5 mm
Reconstruction kernel	B30f

Contrast	
Volume	80 mL
Flow rate	4 mL/s
Volume saline	40 mL

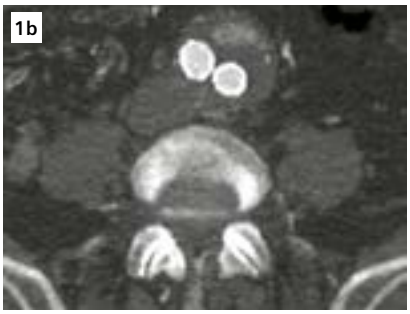

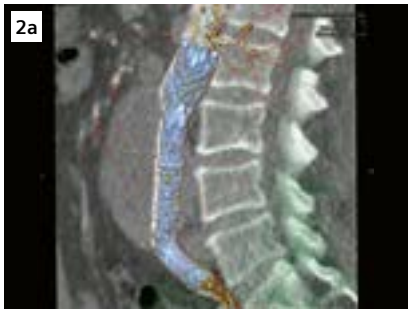

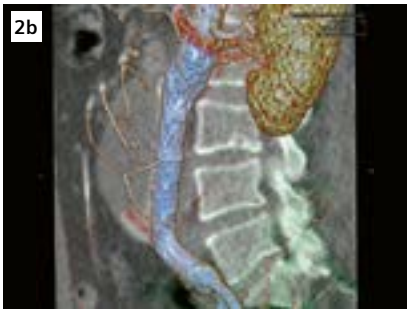

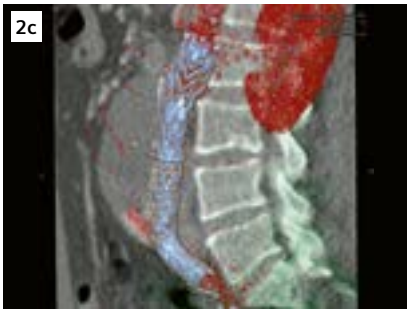

1-2 **Axial (Fig. 1) and VRT (Fig. 2) images showing the different points in time after reaching the bolus tracking threshold.**

(Fig. 1a / 2a) 12 s p. t.: significantly enhanced stentgraft, no endoleak visible.

(Fig. 1b / 2b) 17 s p. t.: well-enhanced stentgraft, and a type IIA endoleak in the ventral aneurysm sac could be visualized.

(Fig. 1c / 2c) 32 s p. t.: no longer enhanced stentgraft, however a well-enhanced endoleak.

3 **Relative time density curves in the aorta (curve 1, yellow), the endloleak (curve 3, orange) and the aneurysm sac (curve 2, green) together with the respective cross-sections where the ROIs were placed: aorta (Fig. 3b), endoleak (Fig. 3c), aneurysm sac (Fig. 3d).**

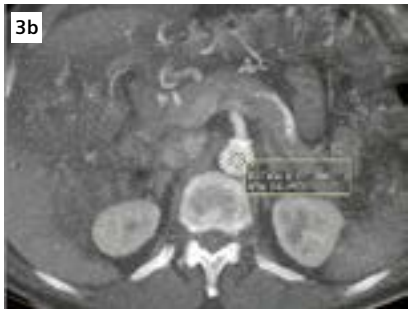

Isolated common iliac artery aneurysm – complicated by peripheral artery insufficiency in the lower limb?

Shufang Cheng, MD; JianSong Ji, MD; Xi Zhao, MD[1]
Department of Radiology, Lishui Central Hospital, The No. 5 Affiliated Hospital of Wenzhou Medical College, Lishui, Zhejiang, P. R. China
[1]Siemens Healthineers, China

History

An 80-year-old male patient, complaining of chest discomfort, shortness of breath and lower limb edema, came to the hospital for a checkup. A Dual Energy (DE) CT angiography (CTA), followed by a dynamic 4D CTA were performed for evaluation.

Diagnosis

CTA images revealed an isolated aneurysm in the right common iliac artery (RCIA). It extended from the aortic bifurcation to the proximal right external iliac artery (REIA), with a maximum diameter of 4.1 cm. Severe stenoses in the proximal left renal artery (LRA) and the left internal iliac artery (LIIA) were seen. Extensive calcified plaques in multiple abdominal and peripheral arteries, causing mild to moderate stenoses, were also visualized. Peripheral artery insufficiency was ruled out by dynamic 4D CTA, however, severe stenosis in the right posterior tibial artery (RPTA), caused by calcified plaques, was confirmed. Subsequent percutaneous implantation of endovascular stent-grafts was successfully performed in the aortic bifurcation and in the proximal LRA, and the patient's symptoms were significantly improved.

Examination Protocol

Scanner	**SOMATOM Force**	
Scan area	Runoff	Upper femur to toes
Scan mode	Dual Source Dual Energy	Adaptive 4D Spiral
Scan length	1,294 mm	796 mm
Scan direction	Cranio-caudal	Shuttle
Scan time	3.6 s	21 s
Tube voltage	70 / Sn150 kV	80 kV
Effective mAs	136 / 47 mAs	35 mAs
Dose modulation	CARE Dose4D	CARE Dose4D
$CTDI_{vol}$	2.99 mGy	6.46 mGy
DLP	399.4 mGy*cm	493 mGy*cm
Rotation time	0.28 s	0.25 s
Pitch	0.6	–
Slice collimation	192 × 0.6 mm	48 × 1.2 mm
Slice width	1.5 mm	1.5 mm
Reconstruction increment	1.0 mm	1.0 mm
Reconstruction kernel	Qr40 (ADMIRE 3)	Br36 (ADMIRE 3)
Contrast	320 mg/mL	320 mg/mL
Volume	90 mL + 40 mL saline	35 mL + 35 mL saline
Flow rate	5 mL/s	3.5 mL/s
Start delay	Bolus tracking with 100 HU at the popliteal artery + 5 s	Same as CTA trigger time

1 A cinematic VRT image shows an overview of the complete scan range.

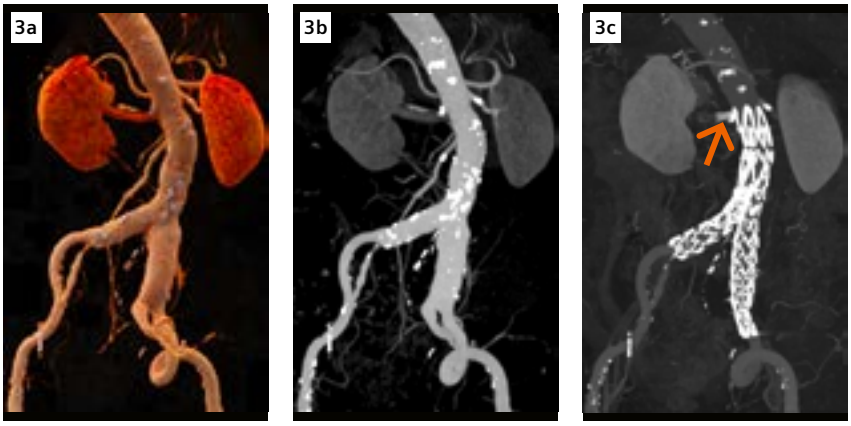

3 Right-posterior views of pre- (Fig. 3a, cVRT; Fig. 3b, MIP) and post- (Fig. 3c, MIP) stenting show an ectatic RCIA, severely stenosed LRA and LIIA, as well as stent grafts in the aortic bifurcation and in the proximal LRA (Fig. 3c, arrow).

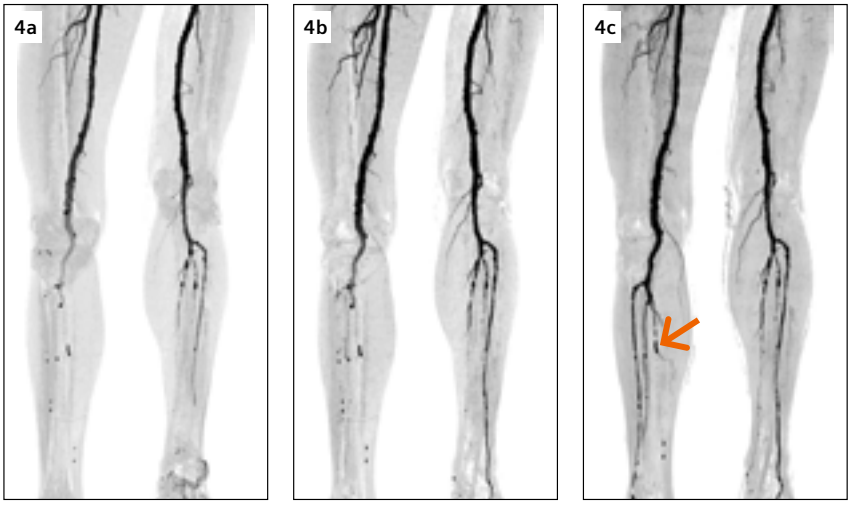

4 A comparison of inverted MIP images (at the same windowing) derived from mixed image (Fig. 4a), mono+50 keV image (Fig. 4b) and dynamic CTA image (Fig. 4c). The peripheral arteries in the lower limbs are best shown in the dynamic 4D CTA, confirming a severe stenosis in the RPTA (arrow).

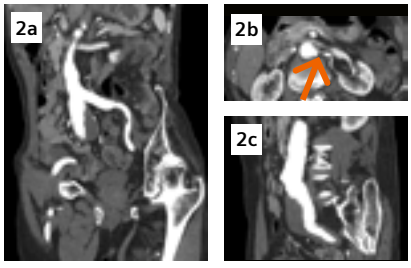

2 MPR images show an aneurysm in the RCIA extending from the aortic bifurcation to the proximal REIA. A severe stenosis of the left renal artery is also seen (Fig. 2b, arrow).

Comments

Isolated aneurysms in the iliac arteries are uncommon and may lead to peripheral artery insufficiency in the lower limbs. Appropriate candidate selection, for endovascular or surgical therapy, greatly relies on imaging classifications. Runoff CTA is usually performed. And DE allows automatic bone removal, as well as significant enhancement of vascular details using *syngo*.CT DE Monoenergetic Plus. However, if the peripheral arteries in the lower limbs are not well shown in DE CTA images, such as in this case, a critical question can be raised – does this indicate peripheral artery insufficiency or missing the bolus? Dynamic 4D CTA is performed using Adaptive 4D Spiral scanning to acquire images at multiple time points with defined intervals. This makes wrong bolus timing highly unlikely. Peripheral arteries are clearly demonstrated using the fused temporal maximum intensity projections (tMIP), which improves diagnostic confidence and helps the physicians making an appropriate treatment plan. ●

CT Volume Perfusion imaging in a case of suspected pancreatic cancer

Sonja Sudarski, MD; Mathias Meyer, MD; Holger Haubenreisser, MD; Stefan O. Schönberg, MD; Thomas Henzler, MD
Institute of Clinical Radiology and Nuclear Medicine, University Medical Centre Mannheim, Medical Faculty Mannheim, Heidelberg University, Germany

History

A 62-year-old male patient presented to the hospital, complaining of persistent upper abdominal pain which was exacerbated after intake of fatty foods. He claimed to have lost 15 kg and to have completely quit consuming alcohol in the past two months. Fatty defecation had not been observed, however, a tendency toward obstipation had developed which could be occasionally relieved by inducing vomiting. The patient had a history of acute pancreatitis, gastrointestinal ulcer bleeding within the duodenum, chronic type B gastritis, and pandiverticulosis. Endosonography results indicated a suspected chronic pancreatitis. Esophagogastroduodenoscopy revealed erosive gastritis, a gastric voiding disorder as well as an axial hiatus herniation. A biphasic CT examination of the chest and abdomen, as well as perfusion imaging of the pancreas, were requested for further evaluation.

Diagnosis

CT images revealed a hypodense lesion, measuring 6.4 × 3.2 cm, in the corpus of the pancreas. The lesion was compressing the portal vein, had infiltrated the splenic vein and reached the coeliac trunk, the common hepatic artery and the gastroduodenal artery. It also surrounded the left gastric artery, and the splenic artery which was constricted by the lesion. Extensive paragastric collaterals were formed.
No suspicious lymph nodes or metastases were seen within the chest and abdomen. Compared with the supposedly healthy and normally perfused tissue of the pancreatic head, the lesion was hypoperfused. MRI confirmed the CT findings, showing a contrast-enhanced lesion with moderate diffusion restriction. The patient underwent surgical exploration and resection. The histopathology revealed local advanced pancreatic adenocarcinoma.

Comments

Organ perfusion CT studies provide anatomical as well as functional information, which is useful for tissue characterization and evaluation of response to therapy.[1] Pancreatic perfusion studies were first performed in the 1990s.[2] However the lack of full organ coverage was the most obvious limitation of this technique, as were the radiation dose concerns that made multiphasic scanning the standard procedure for decades. With the evolution of larger detectors and dose saving strategies, wholeorgan CT perfusion studies are increasingly performed in patients to gain additional functional information.[3] In this case, it was possible to stay within the diagnostic reference dose values for the complete chest, abdominal and volume perfusion CT scans. The CT Body Perfusion application of the *syngo*.via VA30 allows automatic motion correction and noise reduction, as well as the creation of perfusion maps such as blood flow, blood volume, and flow extraction product (permeability). Before finding its way into clinical routine, large studies are needed in order to investigate the robustness of the perfusion parameters and to define possible cut-offs that help to properly interpret the quantitative measurements. ●

References

[1] Cao N, Cao M, Chin-Sinex H, Mendonca M, Ko SC, Stantz KM. Monitoring the Effects of Anti-angiogenesis on the Radiation Sensitivity of Pancreatic Cancer Xenografts Using Dynamic Contrast-Enhanced Computed Tomography. Int J Radiat Oncol Biol Phys. 2014 Feb 1;88(2):412–8. doi: 10.1016/j.ijrobp.2013.11.002.

[2] Miles KA, Hayball MP, Dixon AK. Measurement of human pancreatic perfusion using dynamic computed tomography with perfusion imaging. Br J Radiol. 1995 May;68(809):471–5.

[3] Xie Q, Wu J, Tang Y, Dou Y, Hao S, Xu F, Feng X, Liang Z. Whole-organ CT perfusion of the pancreas: impact of iterative reconstruction on image quality, perfusion parameters and radiation dose in 256-slice CT-preliminary findings. PLoS One. 2013 Nov 26;8(11):e80468. doi: 10.1371/journal.pone.0080468.

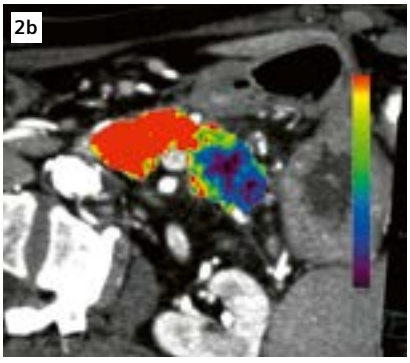

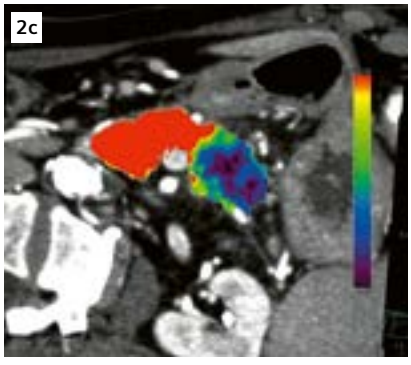

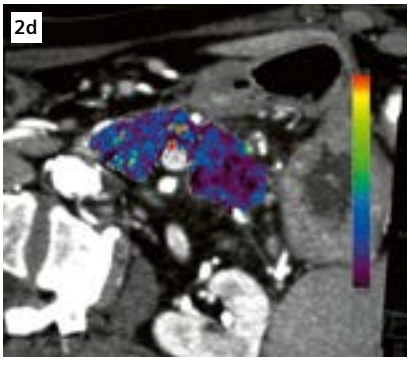

Examination Protocol

Scanner	SOMATOM Force
Scan area	Upper Abdomen
Scan mode	VPCT
Scan length	174 mm
Scan direction	Shuttle
Scan time	43 s
Tube voltage	70 kV
Effective mAs	200 mAs
$CTDI_{vol}$	46.66 mGy
DLP	914.9 mGy*cm
Rotation time	0.33 s
Slice collimation	48 × 1.2 mm
Slice width	1.5 mm
Reconstruction increment	1.0 mm
Reconstruction kernel	Br36
Contrast	400 mg / mL
Volume	50 mL + 50mL saline
Flow rate	5 mL / s
Start delay	5 s

1 **Curved MPR (Fig. 1a) and VRT (Fig. 1b) images show that the lesion was compressing the portal vein, had infiltrated the splenic vein and reached the coeliac trunk, the common hepatic artery, and the gastroduodenal artery. It also surrounded the left gastric artery and the splenic artery which was constricted through the lesion. The extensive paragastric collaterals that were formed can also be seen.**

2 **In comparison with the normal pancreatic tissue, the adenocarcinoma revealed hypodensity in the temporal MIP (Fig. 2a), less blood flow (Fig. 2b), less blood volume (Fig. 2c) and a decreased flow extraction product (Fig. 2d).**

3 **Relative time-density curves (ROI#3 in yellow = normal pancreatic tissue; ROI#4 in green = adenocarcinoma).**

CT imaging of insulinomas – biphasic or dynamic?

Juan Li, MM; Kai Xu, MB; Liang Zhu, MD; Hua-dan Xue, MD; Zheng Yu Jin, MD
Department of Radiology, Peking Union Medical College Hospital, Beijing, P. R. China

History

A 64-year-old female patient, suffering from frequent hypoglycemic attacks, went to a local hospital for a checkup. Clinical and laboratory tests revealed endogenous hyperinsulinemic hypoglycemia. An insulinoma was suspected. A routine abdominal contrast CT was performed, however no tumor was seen. Subsequently, the patient was referred to our institution and a Dynamic CT, covering the liver and the entire pancreas, was performed. The CT data were then used to create different temporal phases and functional parameter maps.

Diagnosis

Perfusion CT images showed an isolated, hyper-perfused lesion in the pancreatic head. The lesion was significantly enhanced in the arterial phase, supplied by the superior pancreaticoduodenal artery, and measured 1.8 × 1.5 cm in size. The non-contrast phase of the liver showed homogeneous hypoattenuation relative to the intrahepatic vessels with a negative liver-to-spleen attenuation ratio. This suggested a diffuse hepatic fat deposition. A hyperdense stone with a hypodense core, measuring 1.9 × 1.5 cm in size, was shown in the gall-bladder. No signs of metastases were seen in the liver or in the adjacent lymph nodes. The patient underwent surgical removal of the tumor, using a laparoscopic approach, and recovered uneventfully.

Comments

Insulinomas are the most common hyperfunctioning pancreatic endocrine tumors.[1] Primarily, the diagnosis is made based on clinical and laboratory findings. Surgical removal of the tumor is the most effective treatment. Preoperative tumor localization using imaging examinations is important,[1–2] especially when a laparoscopic approach for tumor enucleation is considered. According to published data, substantial subsets of insulinomas are not captured in standard biphasic CT scans. This is due to the fact that the enhancement patterns of isolinomas vary and tumorparenchyma contrast is time-dependent. For example, insulinomas which are transient hyperenhancing (30.2%) [3] or isoattenuating (24.9%),[4] can be missed in biphasic CT scans.

In our institution, a low dose dynamic CT scan protocol is employed for imaging suspected insulinomas. The acquired image data is used to evaluate tumor perfusion, as well as to create multiple phases based on the Time-Attenuation Curve (TAC). Image quality is significantly improved using temporal average and temporal MIP reconstructions provided by *syngo*.CT Dynamic Angio. The applied radiation dose is in a range comparable to a biphasic scan plus a native scan.[5] The amount of contrast agent needed is greatly reduced, compared to that of a biphasic protocol, which applies contrast agent according to patients' body weight.[3] In this case (158 cm, 63.5 kg, BMI 25.4), 45 mL was applied instead of 90 mL.

Our experience with this approach has been promising – the required diagnostic information of tumor perfusion, morphology and vascularity can be acquired in a single dynamic scan with comparable radiation dose and a reduced amount of contrast agent. ●

References

[1] Falconi M, Eriksson B, Kaltsas G, et al. ENETS Consensus Guidelines Update for the Management of Patients with Functional Pancreatic Neuroendocrine Tumors and Non-Functional Pancreatic Neuroendocrine Tumors. Neuroendocrinology, 2016, 103(2): 153-171.

[2] Dixon E, Pasieka J L. Functioning and nonfunctioning neuroendocrine tumors of the pancreas. Curr Opin Oncol, 2007, 19(1):30-35.

[3] Zhu L, Wu W, Xue H, et al. Sporadic insulinomas on volume perfusion CT: dynamic enhancement patterns and timing of optimal tumour–parenchyma contrast. European Radiology, 2017, 27(8):3491-3498.

[4] Zhu L, Xue H, Sun H, et al. Isoattenuating insulinomas at biphasic contrast-enhanced CT: frequency, clinicopathologic features and perfusion characteristics. European Radiology, 2016, 26(10):3697-3705.

[5] Zhu L, Xue H, et al. Insulinoma Detection With MDCT: Is There a Role for Whole-Pancreas Perfusion? AJR 2017; 208:306–314 2016, 26(10):3697-3705.

Examination Protocol

Scanner	SOMATOM Force
Scan area	Liver and pancreas
Scan mode	Adaptive 4D Spiral
Scan length	176 mm
Scan direction	Shuttle
Scan time	45 s
Tube voltage	80 kV
Effective mAs	80 mAs
$CTDI_{vol}$	44.14 mGy
DLP	840.3 mGy*cm
Rotation time	0.25 s
Slice collimation	48 × 1.2 mm
Slice width	1.5 / 3 mm
Reconstruction increment	1 / 2 mm
Reconstruction kernel	Br36
Contrast	370 mg / mL
Volume	45 mL + 40 mL saline
Flow rate	5 mL / s
Start delay	6 s

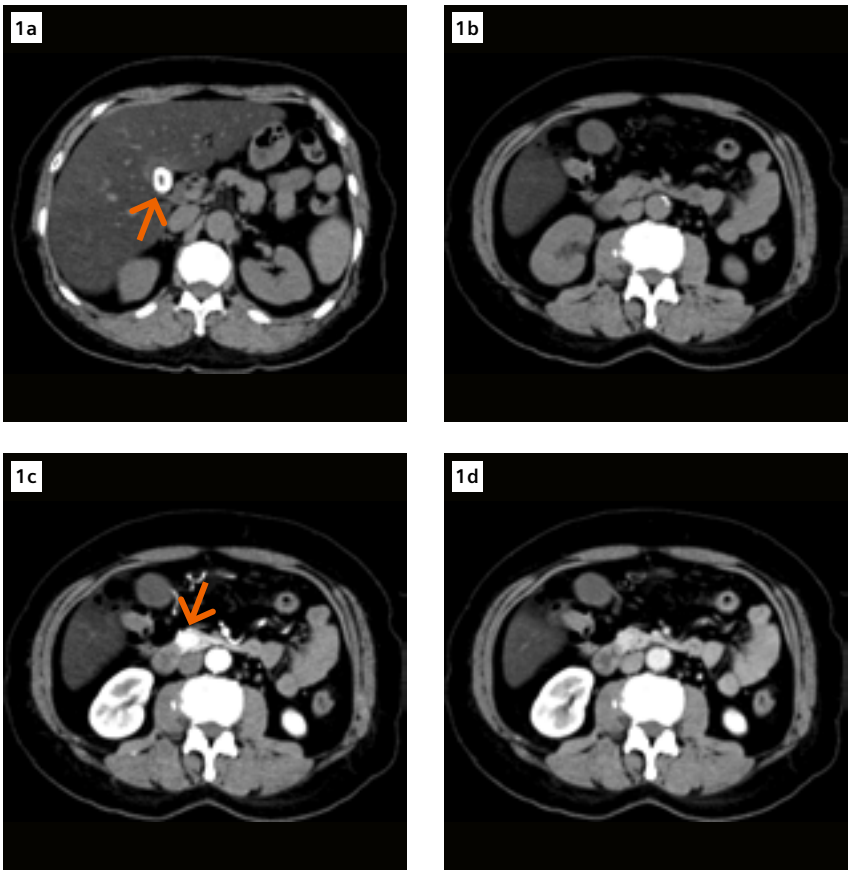

1 Axial CT images (3 mm) of the native (Figs. 1a and 1b), arterial (Fig. 1c) and portal venous (Fig. 1d) phases, created using temporal average reconstruction with *syngo*.CT Dynamic Angio, demonstrate excellent image quality. The liver shows homogeneous hypoattenuation in the native phase (Fig. 1a) relative to the intrahepatic vessels with a negative liver-to-spleen attenuation ratio. This suggests a diffuse hepatic fat deposition. A hyperdense stone (Fig. 1a, arrow) with a hypodense core is shown in the gallbladder. A hyperenhanced lesion (Fig. 1c, arrow) in the pancreatic head is clearly visualized in the arterial phase.

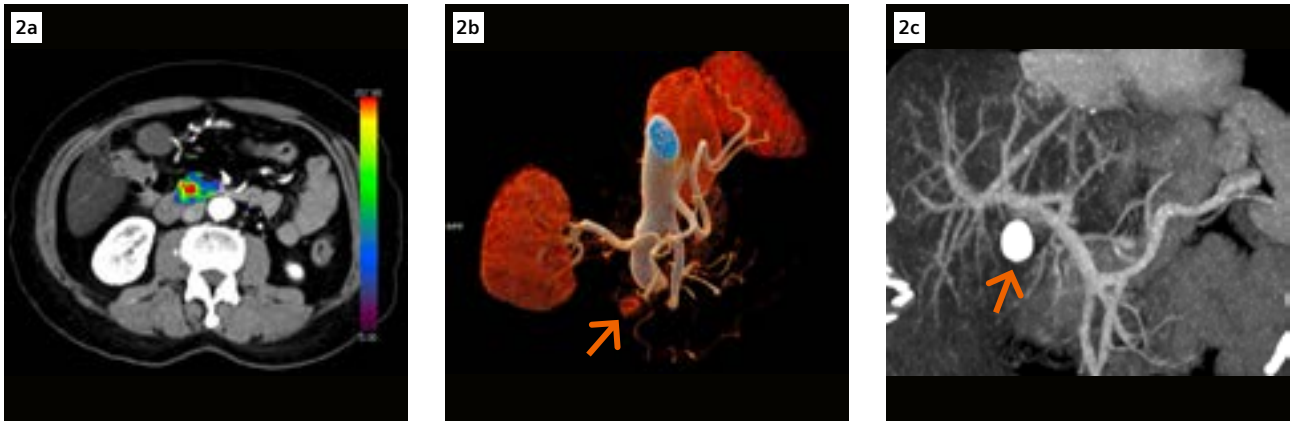

2 CT Perfusion image (Fig. 2a) shows a hyperperfused lesion with higher Blood Flow, compared to the normal pancreatic tissues, in the pancreatic head. A cinematic VRT image (Fig. 2b) demonstrates tumor blood supply (arrow) from the superior pancreatico-duodenal artery. A MIP image (Fig. 2c) shows a normal portal venous system and a hyperdense gallbladder stone (arrow). The arterial and the portal venous phases were created using temporal MIP reconstruction with *syngo*.CT Dynamic Angio.

Pre-operative detection of an isoattenuating pancreatic insulinoma in Volume Perfusion CT

Hua-dan Xue, MD; Liang Zhu, MD; Ping Li, MS; Xi Zhao, MD[1]; Zheng Yu Jin, MD
Department of Radiology, Peking Union Medical College Hospital, Beijing, P. R. China
[1]Siemens Healthineers, China

History

A 23-year-old female patient, suffering from frequent hypoglycemic attacks, was referred to our institution for suspected hyper-functioning pancreatic endocrine tumor. Clinical and laboratory tests suggested endogenous hyper-insulinemic hypoglycemia. Because previous imaging was unable to localize the tumor, Volume Perfusion CT (VPCT) of the pancreas was ordered by the clinician for insulinoma localization.

Diagnosis

Images acquired by Adaptive 4D Spiral scans were reconstructed in multiple series. Dynamic scans captured the transient hyper-enhancement of the tumor – a hyperenhancing nodule with clear margin in the early arterial phase, washing out quickly and becoming isoenhancing compared to the pancreatic parenchyma in the standard pancreatic arterial phase. The hypervascular nature of the tumor was also reflected by its significantly increased perfusion. On the pseudocolored perfusion maps, the tumor was shown as a "hot spot", standing out from the background parenchyma.

Comments

Insulinoma is the most common hyper-functioning pancreatic endocrine tumor. Its characteristic manifestation leads to clinical diagnosis. The role of imaging is to detect and to indicate the precise location of the tumor. Since most insulinomas are small, and the changes of pancreatic contour are subtle or absent, tumor localization greatly relies on the enhancement pattern.[1,2] Although insulinomas typically manifest as a hyperenhancing nodule, isoattenuating tumors can be encountered in up to 25% of the cases,[3] which limits the sensitivity of standard biphasic enhanced CT.[4] VPCT of the pancreas allows for fast, dynamic scans of the pancreas, which are useful in capturing the transient hypervascular flush of the tumors. Since isoattenuating tumors show significant increased blood flow compared to the normal pancreatic parenchyma, VPCT may increase the sensitivity for insulinoma detections. ●

References

[1] Liu Y, Song Q, Jin HT, Lin XZ, Chen KM (2009) The value of multidetector-row CT in the preoperative detection of pancreatic insulinomas. Radiol Med 114:1232–1238.

[2] Daneshvar K, Grenacher L, Mehrabi A, Kauczor HU, Hallscheidt P (2011) Pre-operative tumor studies using MRI or CTin patients with clinically suspected insulinoma. Pancreatology 11:487–494.

[3] Liang Zhu, Hua-dan Xue, Hao Sun, XuanWang, Yong-lan He, Zheng-yu Jin, Yu-pei Zhao Isoattenuating insulinomas at biphasic contrast-enhanced CT: frequency, clinicopathologic features and perfusion characteristics. European Society of Radiology, published online 26 Jan. 2016.

[4] Fidler JL, Fletcher JG, Reading CC et al (2003) Preoperative detection of pancreatic insulinomas on multiphasic helical CT. AJR Am J Roentgenol 181:775–780.

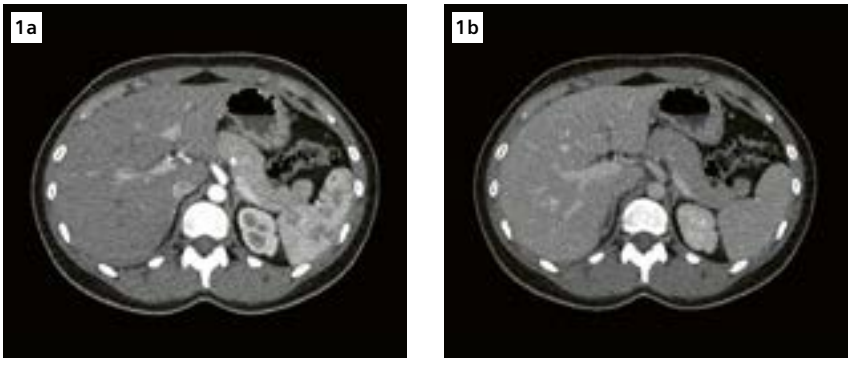

1 **Arterial (Fig. 1a) and portal venous (Fig. 1b) phases of previous CT revealed negative result.**

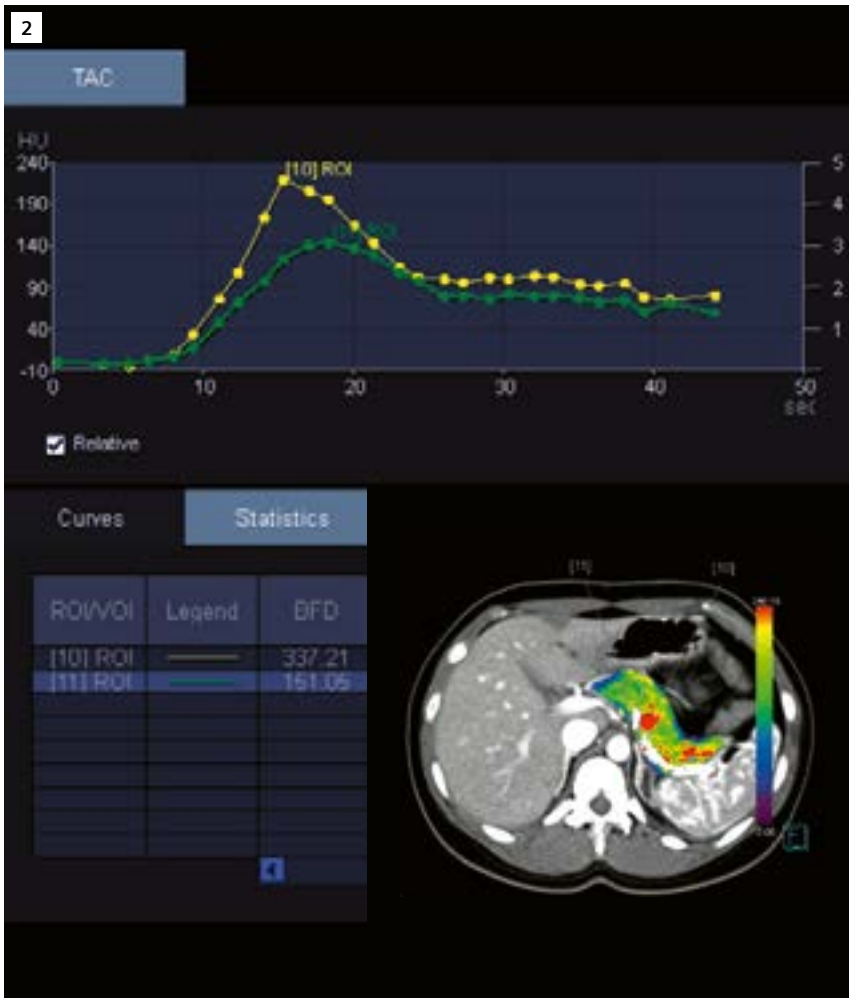

2 **The tumor-harbouring area (ROI#10) shows more than doubled blood flow than that of the tumor-free area (ROI#11).**

Examination Protocol

Scanner	**SOMATOM Force**
Scan area	Upper abdomen
Scan mode	Adaptive 4D Spiral
Scan length	176 mm
Scan direction	Shuttle
Scan time	43.5 s
Tube voltage	80 kV
Effective mAs	55 mAs
$CTDI_{vol}$	30.3 mGy
DLP	577 mGy*cm
Effective dose	8.7 mSv
Rotation time	0.325 s
Slice collimation	48 × 1.2 mm
Slice width	3 mm
Reconstruction increment	2 mm
Reconstruction kernel	Br36
Contrast	370 mg / mL
Volume	48 mL + 20 mL saline
Flow rate	5 mL / s
Start delay	6 s

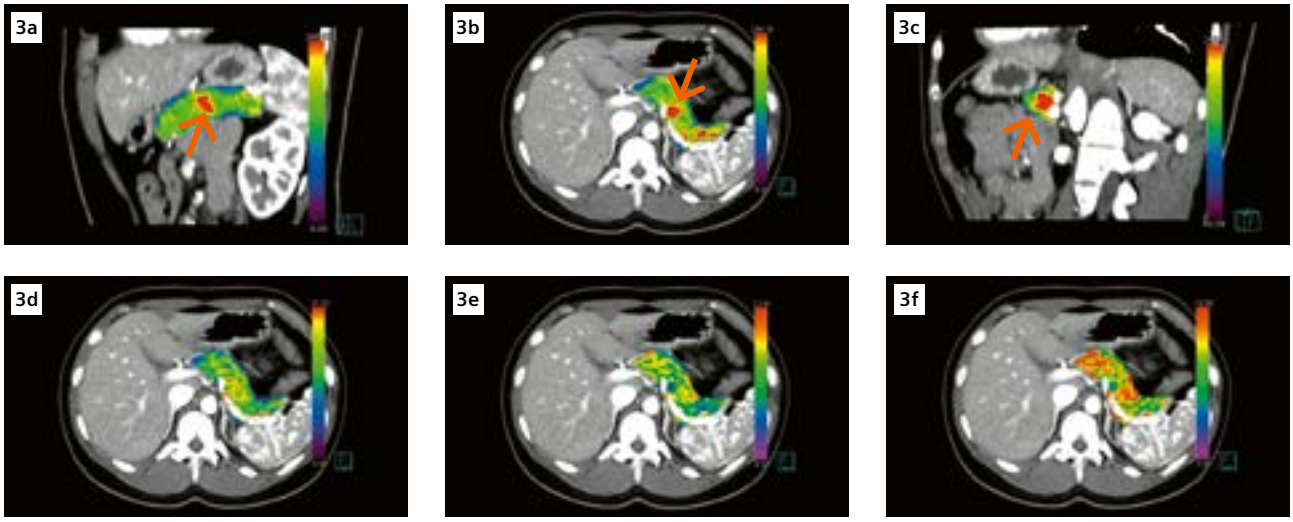

3 **Perfusion maps show a higher blood flow (BF, arrows, Fig. 3a – long axis, Fig. 3b – axial, Fig. 3c – short axis), an inconspicuous blood volume (BV, Fig. 3d), a shorter mean transit time (MTT, Fig. 3e) and a shorter Tmax* (Fig. 3f).**

** Time needed by a theoretical unit of contrast media to reach the maximum concentration in one specific voxel. Mathematically defined as Tmax = TTS + MTT/2. It reflects the transit time to the center of the IRF (ideal impulsive bolus response function) at the voxel location. Tmax is the sum of the arteries' bolus delay and the tissue.*

Volumetric Perfusion CT for early assessment of response to anti-angiogenic therapy in metastatic renal cell carcinoma

Alexander Sterzik, MD; Melvin D'Anastasi, MD; M. Staehler, MD; Maximilian Reiser, MD; Anno Graser, MD
Departments of Clinical Radiology and Urology, Campus Grosshadern, University Hospital Munich, Germany

History

A 46-year-old male patient, with a right-sided partial nephrectomy due to papillary renal cell carcinoma one year ago, presented with tumor recurrence and new metastases in the right paracolic gutter and right abdominal wall. He was scheduled for anti-angiogenic tyrosin-kinase-inhibitor (TKI) therapy. Serial volumetric perfusion-CT scans of a selected representative metastatic lesion were performed, before as well as seven days after commencement of the anti-angiogenic TKI therapy, for noninvasive monitoring of early treatment response.

Diagnosis

Volumetric perfusion CT analysis of the assessed target lesion, in the right paracolic gutter (Fig. 1), showed increased baseline levels of tumor blood flow (BF), blood volume (BV) and vessel permeability (PMB) as features of tumor angiogenesis (Fig. 2a). A further perfusion CT scan performed after one week of TKI treatment which revealed a remarkable reduction in tumor perfusion indices (Fig. 2b) with a reduction in BF, BV and PMB levels of 70–80%, compared to their respective baseline values. On the other hand, tumor volume increased from about 53 mL (pre-treatment) to 89 mL (post-treatment) due to substantial tumor necrosis (Fig. 1). Based on the information from the perfusion CT scan, treatment was continued – despite the substantial increase in tumor size. Under ongoing TKI therapy, the patient is still in stable disease without further tumor growth (18 months after therapy begin).

Comments

With the introduction of anti-angiogenic therapy as a standard treatment in patients with metastatic renal cell carcinoma, new diagnostic challenges arise in the assessment

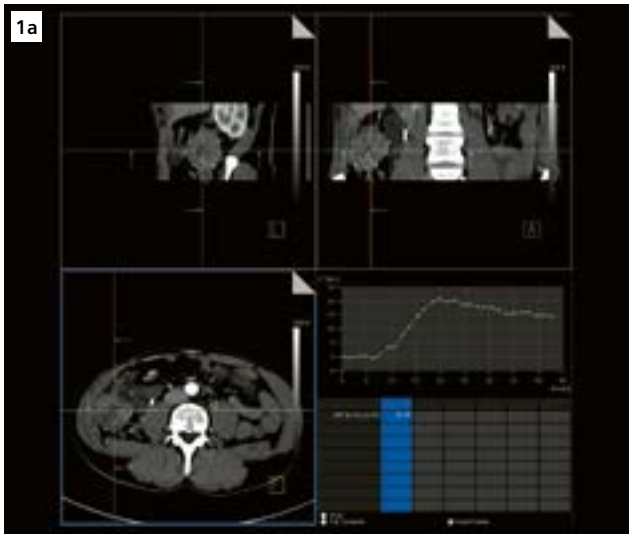

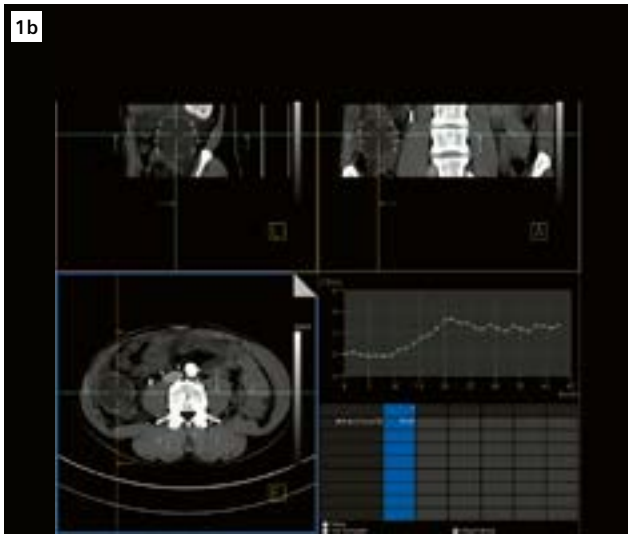

1 **Temporal MIP images of two serial perfusion CT scans centered around the metastatic target lesion in the right paracolic gutter, covering the entire tumor volume. After one week of TKI therapy, tumor volume increased from about 53 mL before therapy begin (Fig. 1a) to 89 mL post-treatment (Fig. 1b). However, as indicated by the time-resolved enhancement curves in the lower right quadrant of each figure, the contrast uptake within the tumor tissue had been reduced dramatically on day 7. Please note different scale of y axis in Figs. 1a and 1b.**

of therapeutic efficacy. Large clinical studies have shown that classical response criteria such as RECIST, which only take into account changes in tumor size, are of limited use in predicting long-term outcome in patients with metastatic renal cell carcinoma (mRCC).[1–3] This is – given the cytostatic rather than cytotoxic profile of anti-angiogenic agents – not unexpected. Functional imaging techniques, which quantitatively assess tumor perfusion such as perfusion CT, are currently being investigated as new biomarkers for predicting a response to anti-angiogenic therapy in cases of mRCC.[4] As changes in tumor vascularity precede morphological changes, perfusion CT may have the potential to aid physicians in evaluating therapeutic response in patients with mRCC at an early stage. This case nicely illustrates that perfusion CT can depict therapy-induced changes in tumor vascularity, as early as 7 days after commencing anti-angiogenic treatment. Whether CT-perfusion imaging can be a valuable adjunct to monitor response and aid physicians in predicting the outcome of anti-angiogenic therapy, must be evaluated in further studies. Considering the broad dissemination profile of mRCC, with possible tumor manifestations to virtually all organs, the assessment of tumor perfusion in this tumor entity is challenging. With its integrated motion correction and semi-automated tumor segmentation algorithms – automatically excluding intratumoral vessels or bony structures from the analysis – VPCT software is a versatile tool for quantitative analysis of volumetric CT-perfusion data of patients with systemic tumor manifestations such as mRCC. ●

References

[1] Motzer, R.J., et al., Pazopanib versus sunitinib in metastatic renal-cell carcinoma. N Engl J Med. 369(8): p.722-31.

[2] Motzer, R.J., et al., Sunitinib versus interferon alfa in metastatic renal-cell carcinoma. N Engl J Med, 2007. 356(2): p.115-24.

[3] Sternberg, C.N., et al., Pazopanib in locally advanced or metastatic renal cell carcinoma: results of a randomized phase III trial. J Clin Oncol. 28(6): p.1061-8.

[4] Braunagel, M., et al., The role of functional imaging in the era of targeted therapy of renal cell carcinoma. World J Urol. 32(1): p. 47-58.

Examination Protocol

Scanner	**SOMATOM Definition Flash**
Scan area	Mid abdomen
Scan length	100 mm
Scan mode	Adaptive 4D Spiral
Scan direction	Shuttle
Scan time	44 s
Tube voltage	100 kV
Effective mAs	120 mAs
$CTDI_{vol}$	125.83 mGy
DLP	1483.6 mGy*cm
Effective dose	22 mSv
Rotation time	0.28 s
Slice collimation	32 × 1.2 mm
Slice width	3 mm
Reconstruction increment	2 mm
Reconstruction kernel	B20f
Contrast	300 mg / mL
Volume	50 mL + 50 mL saline
Flow rate	6 mL / s
Start delay	8 s

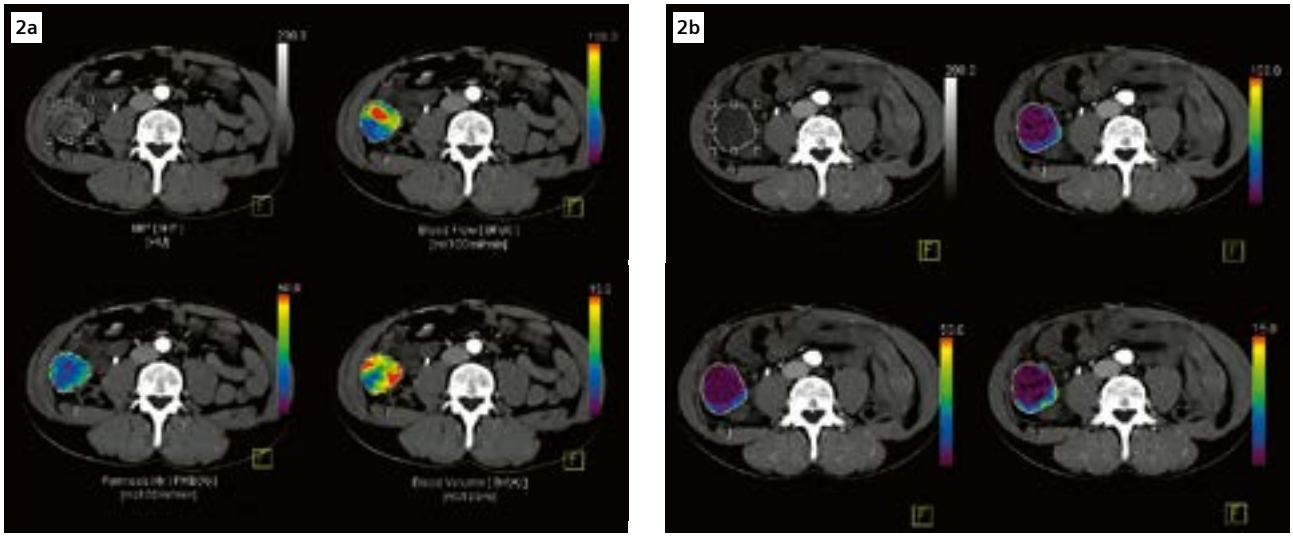

2 Axial semi-quantitative color-coded VPCT parameter maps of the tumor perfusion indices (tumor blood flow, tumor blood volume and vessel permeability), acquired before treatment begin, depict regional heterogeneity of tumor vascularity with a mixture pvascular (colored in red) and hypovascular (colored in blue) areas (Fig. 2a). After 7 days of TKI therapy, the tumor has become almost completely hypovascular showing only small spots with residual perfusion (Fig. 2b).

Volume Perfusion CT during hepatic arteriography of hepatocellular carcinoma

Yoshiaki Katada, MD, PhD; Shingo Watanabe
Department of Radiology, Dokkyo University Koshigaya Hospital, Koshigaya, Japan

History

A 78-year-old male patient, suffering from a hepatocellular carcinoma (HCC, TNM stage A and BCLC stage A), was scheduled for trans-arterial chemo embolization (TACE).
CT scans were requested to confirm the location and size of the tumor prior to intervention.

Diagnosis

A non-contrast CT (Fig. 1a) as well as a CT arterial portography (CTAP, Fig. 1b) were routinely performed. A low density lesion, measuring 1.8 cm, was seen in the right hepatic lobe, segment VIII. Further contrast media was then injected through a catheter that was advanced into the right hepatic artery (RHA), to perform a Volume Perfusion CT (VPCT, Fig. 2) and a CT hepatic arteriography (CTHA, Fig. 3). Both scans confirmed that the lesion was hypervascularized with a much higher blood flow than that of the normal liver tissue. TACE was successfully performed afterwards.

Comments

VPCT is a useful diagnostic tool for oncology cases. That it can also be performed during interventions, such as TACE, is a definite advantage for the patient. Advancing the catheter into the RHA, the contrast bolus can be injected intensively into the right lobe. Thus, the lesion can be greatly enhanced with much less contrast media and radiation dose (in this case only 8 mL and 30 mAs). It is worthwhile to note that the liver model which was defined for hepatic vascular system with dual blood supply (arterial and portal venous) is not suitable here. In a case like this, the tumor model should be applied for perfusion evaluation instead. ●

Examination Protocol

Scanner	**SOMATOM Definition**
Scan area	Liver
Scan length	154 mm
Scan mode	Adaptive 4D Spiral
Scan direction	Shuttle
Scan time	35 s
Tube voltage	120 kV
Effective mAs	30 mAs
$CTDI_{vol}$	31.8 mGy
DLP	519 mGy*cm
Effective dose	7.8 mSv
Rotation time	0.33 s
Slice collimation	24 × 1.2 mm
Slice width	3 mm
Reconstruction increment	2 mm
Reconstruction kernel	B30f
Contrast	150 mg / mL
Volume	8 mL
Flow rate	2 mL / s
Start delay	No

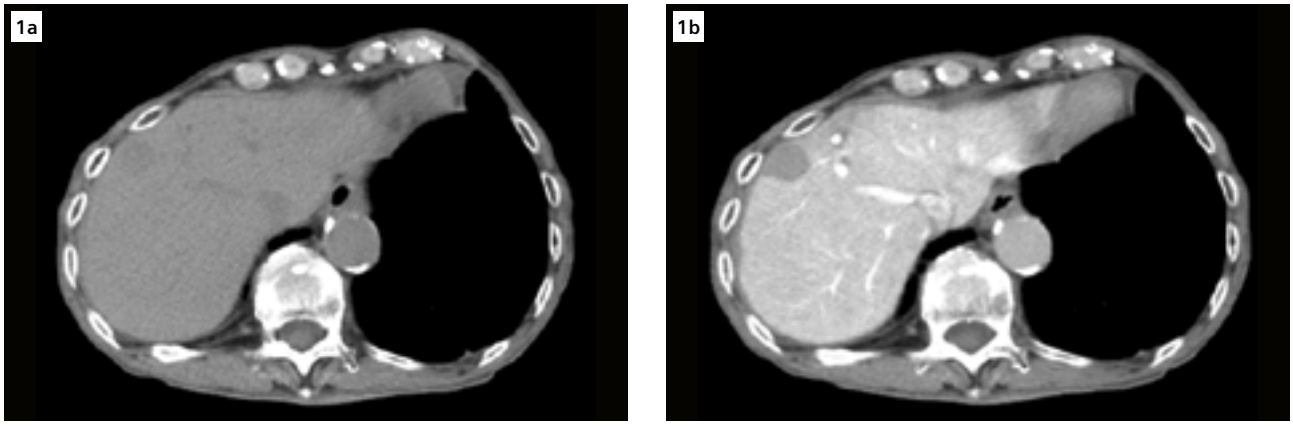

1 Non-contrast CT (a) and CTAP (b) show a low density lesion measuring 1.8 cm in the right hepatic lobe, segment VIII.

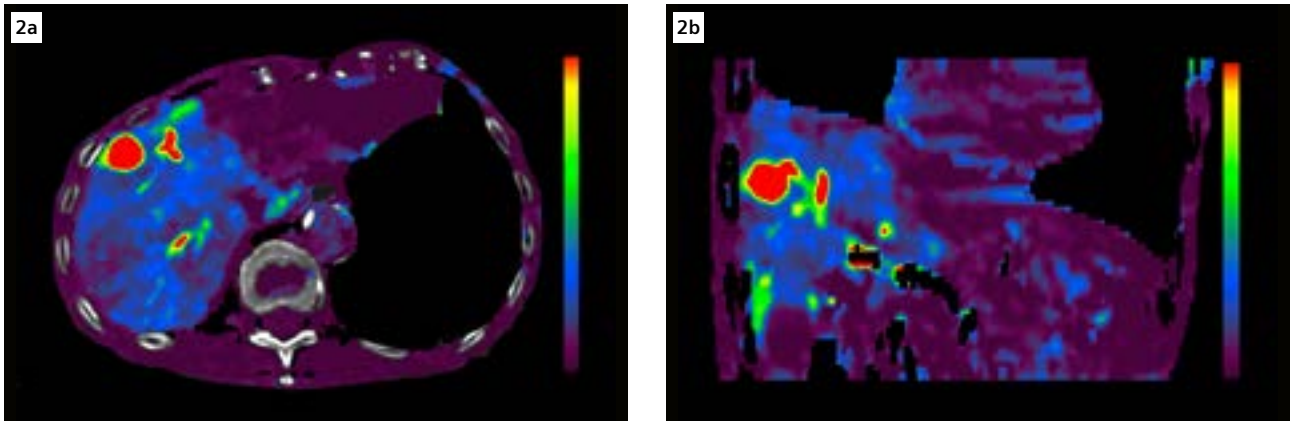

2 An axial (a) and a coronal (b) image of VPCT show the lesion (in red) with a much higher blood flow than that of the rest normal tissue. Note that only the right hepatic lobe is perfused since the contrast was injected directly into the RHA.

3 CTHA images characterize the so-called "fast in, fast out" patent of the hepatic tumor – in comparison with that of the normal liver tissue, the enhancement of the lesion appeared earlier (a, b) and withdrew earlier as well (c).

Legal information: On account of certain regional limitations of sales rights and service availability, we cannot guarantee that all products included in this brochure are available through the Siemens Healthineers sales organization worldwide. Availability and packaging may vary by country and is subject to change without prior notice. Some/All of the features and products described herein may not be available in the United States.

The information in this document contains general technical descriptions of specifications and options as well as standard and optional features which do not always have to be present in individual cases.

Siemens Healthineers reserves the right to modify the design, packaging, specifications, and options described herein without prior notice. Please contact your local Siemens sales representative for the most current information.

Note: Any technical data contained in this document may vary within defined tolerances. Original images always lose a certain amount of detail when reproduced.

The statements and outcomes by Siemens Healthineers customers described herein are based on results that were achieved in the customer's unique setting. Since there is no "typical" hospital and many variables exist (e.g., hospital size, case mix, level of IT adoption) there can be no guarantee that other customers will achieve the same results.

In clinical practice, the use of ADMIRE may reduce CT patient dose depending on the clinical task, patient size, anatomical location, and clinical practice. A consultation with a radiologist and a physicist should be made to determine the appropriate dose to obtain diagnostic image quality for the particular clinical task.

International version.
Not for distribution or use in the U.S.

Siemens Healthineers Headquarters
Siemens Healthcare GmbH
Henkestr. 127
91052 Erlangen, Germany
Phone: +49 9131 84-0
siemens-healthineers.com

Published by Siemens Healthcare GmbH · 9499 1120 · online ·